Computational Research Progress in Applied Science & Engineering
©PEARL publication, 2017

ISSN 2423-4591

CRPASE Vol. 03(03), 115-122, September 2017

Numerical Modelling of Size Effect on Subgrade Reaction Modulus Using DEM

Hadi Ahmadi[a*], Saman Farzi Sizkow[b]

[a] *Department of Civil Engineering, University of Guilan, Iran*
[b] *School of Civil and Environmental Engineering, Amirkabir University of Technology, Iran*

Keywords

Size effect,
Modulus of subgrade reaction,
Discrete element method,
Uniform sand,
Plate load test.

Abstract

In the flexible foundation analysis theories, such as beam on elastic foundation and Winkler's model, the modulus of subgrade reaction is proposed as the soil's resilience coefficient in a semi-infinite environment. The modulus of subgrade reaction is usually determined in field-study form and through the plate loading test. One of the influential parameters in the modulus of subgrade reaction is the size of the particles and aggregates. The present research has evaluated the effect of particle size on the modulus of subgrade reaction using numerical simulation and discrete element method. To this aim, samples with completely identical granulation conditions as well as samples with relatively uniform granulation, having finite particle range were modeled in different sizes and stress-displacement variations were measured in them through the discrete element method. Given the uniformity of type and shape of the aggregates, the results of the numerical modeling show that the medium size has a direct relationship with the modulus of subgrade reaction of the sand; specifically, in the high percentage density, increase in size of the aggregates greatly increases the modulus of subgrade reaction. These variations are almost linear in completely uniform aggregates and show a relatively logarithmic process in samples with a limited size range.

1. Introduction

The modulus of subgrade reaction implies the elastic behavior of the soil under loading by flexible foundation. This parameter is generally defined by the results of plate load test as follows

$$K_S = \frac{q}{s} \quad (1)$$

where q and s are the stress on the plate and vertical deformation of the rigid plate, respectively [1]. In flexible foundation analysis theories, such as the beam on elastic foundation and Winkler's model, the modulus of subgrade reaction is proposed as the soil's resilience coefficient in a semi-infinite environment [2]. This parameter is generally determined using the plate load test and based on ASTM D1194 standard. Biot presented an experimental relationship for the modulus of subgrade reaction wherein the mentioned coefficient depends on elastic parameters, stiffness of the loaded beam and the underlying soil [3]. Terzaghi has evaluated the modulus of subgrade reaction and the conditions influential in employing it to interfere the flexibility of foundation on the soil. The role of parameters such as shape of the plate, flexibility and also the depth of its deployment in the reaction module has been studied. Terzaghi showed that the modulus of subgrade reaction is reduced with increase in width of the plate [4]. Selvadurai has studied the loading effect zone in a flexible plate [5]. Also, Vesic' has studied the geometric effect of loading on the modulus of subgrade reaction [6]. Makhlouf and Stewart have evaluated the factors affecting the stiffness and elasticity modulus of the dry sand [7]. Okeagu and Abdel-Sayed have conducted a study on determining the factors affecting normal modulus of subgrade reaction for the flexible surface conduits [8]. Also, some analyses have been done using the finite element method under this condition. The results obtained by these researchers showed that the soil reaction coefficients significantly depend on loading conditions, the distance between the openings, depth of the soil and loading direction. Ismael has studied the coefficient of subgrade reaction on desert sand for the flexible footing [9]. Lin et al., have also evaluated the modulus of subgrade reaction and stiffness features of the sandy coarse-aggregated soils in form of studying the deformability behavior [10]. Daloglu, and Vallabhan proposed a method to evaluate the equal modulus of subgrade reaction for use in Winkler's model [11]. That study has proposed graphs

* Corresponding Author:
E-mail address: hadiahmadi@guilan.ac.ir

Received: 12 June 2017; Accepted: 18 September 2017

through which value of the equivalent subgrade reaction modulus can be determined using the geometric characteristics and system's condition. Moayedi and Naeini have evaluated the subgrade reaction modulus in gravely soils based on the results from the in-situ Standard Penetration Test (SPT) [12]. The results which have been conducted on coarse-aggregated sediments of Tehran show the relationship among the two in-situ tests of SPT and PLT. Dey and Basudhar (2008) investigated flexible behavior of the beams and the foundations on a coarse sandy bed. In those studies, the role of K_s in flexible foundations was analyzed based on Winkler's spring theory and the standard four-element viscoelastic Burger model [13]. Meshkat (2007) has evaluated the influence of loading scale and direction on response coefficient of the foundation using the plate load test [14]. Also, Ahmadi and Meshkat (2008) have studied the subgrade reaction modulus variations with foundation's dimensions and proposing a relationship for Tehran's soil using the plate load test [15].

Present research tries to evaluate the influence of size of granular soil particles on the subgrade reaction modulus and soil stiffness by analyzing the soil's granular behavior. To this aim, the discrete element method was used and the results from numerical simulation were validated using the results of the physical modeling done on Anzali sand.

2. Discrete Element Method

Discrete Element Method (DEM) is a set of numerical techniques specifically used to model the behavior of the discrete systems such as the granular environments. Discrete element method was first introduced by Cundall in 1971 [16] to simulate the behavior of the interlocking rocks and then developed by Cundall and Strack in 1979 [17] for the granular products. In recent years, use of discrete element method to simulate the microstructure behavior of the granular materials such as sand has been greatly expanded. Especially, many improvements have been made in simulating the laboratory tests such as direct shear test [18-20], triaxial test [21, 22], true triaxial test [23], cycle triaxial test [24], cycle loading [25], hollow cylindrical torsional test [26] and oedometer consolidation test [27]. In other geothechnical issues, researches by Cleary and Campbel (1993), He et al. (2010) and Jiang and Murakami (2012) in analysis of landslide and stability of the grider [28], Cleary (2000) in analysis of excavation [29], as well as El Shamy and Zamani (2011) [30] to investigate the seismic response of the surface foundations considering the soil-foundation-structure interaction [30], can also be mentioned.

A discrete element simulation system is generally composed of four main components including component display, call detection, physics and visualization [31]. compared to finite element and finite volume methods, discrete element method is a non-mesh method which solves the numerical problems considering mechanical properties of a particle and mathematical calculations on it. Interaction between the components is done only through the contact points. Thus, little equations must be solved for each element. Therefore, forces and displacements for each particle wherever in the system can be followed and examined separately. But, due to very large number of the particles for a real problem modelling and therefore, the very high operating volumes, it is often not possible to take actual dimensions for a particle and different parameters of the problem will have changes in scale. In the analysis using the discrete element method, two basic rules will govern:

1. The law of motion (Newton's second law),
2. Force displacement law.

The law of motion applies to every particle and includes force and momentum. The force displacement law is applied to every contact and observes the rules of continous environments while obsrving the relative motion. The contact forces can be solved in form of Fn normal forces and Fs tangent forces in equilibrium equations through providing a resistence by locating a set of springs and dampers. There are several models for analyzing the contact mechanics. The linear and contact model of Hertz-Mindelin are appropriate models for non-cohesive granular materials and these models are used for many of the discrete element method codes for such issues. Figure 1 shows the components of linear model (a) and Hertz-Mindelin contact model (b) schematically. The linear method is in fact the extention of Hertz-model by Cundall (1979) which is a simple and quick solution in the calculations. In this model, relative forces and displacements are associated by the fixed contact stiffness among the two particles. While in Hertz-Mindelin contact model, the relative forces and displacements establish a non-linear connection in form of unstable contact stiffness which is a function of geometric properties and type of the materials and the connection is made by placing a series of springs and dampers in the contact area.

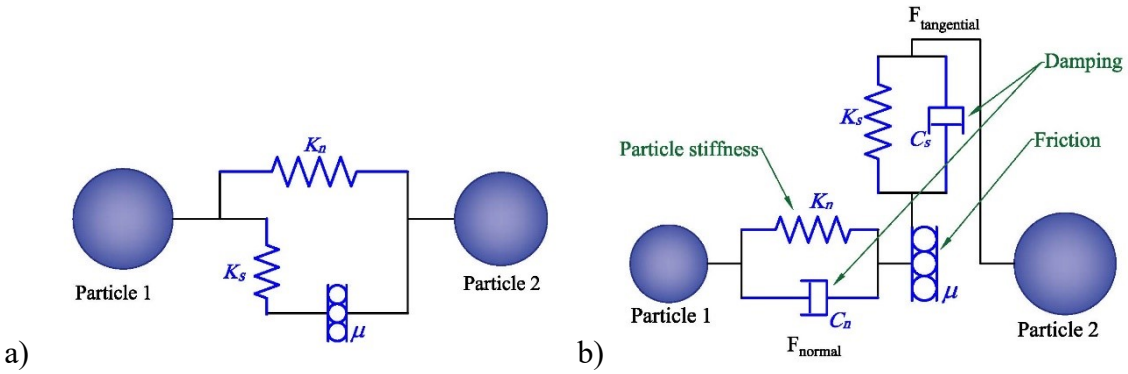

Figure 1. Schematic view of the components of linear model (a) and Hertz-Mindelin contact model (b)

3. Formulation of Discrete Elements

In the studied environment, the sand particles are under the gravity forces and the contact forces among the particles. Hence, the equations of motion and momentum are defined in Eqs. (2) and (3) to describe the motion of a discrete particle [32]

$$m_p \ddot{u}_p = m_p a_g + \sum_{c=1}^{N_{cp}} f_c \quad (2)$$

$$I_p \ddot{\theta}_p = \sum_{c=1}^{N_{cp}} r_c \times f_c \quad (3)$$

where $\ddot{u}_p$ is the transitional displacement, $\ddot{\theta}_p$ is the rotational displacement and m_p is mass of the *p*th particle, f_c is the interparticle force, r_c is the distance from center of the mass to the contact point at the *c*th contact surface and N_{cp} is the number of contacts around the particles. Also, a_g is the gravitational acceleration vector. The interparticel force at contact is consisted of two components of normal and tangential (shear) and can be written as Eq. (4)

$$f_p = f_p^n + f_p^s \quad (4)$$

where f_p^n and f_p^s are the normal and shear components of the interparticle force, respectively which are obtained from the following relations

$$df^n = (K^n du^n + C^n d\dot{u}^n)n \quad (5)$$

$$df^s = (K^s du^s + C^s d\dot{u}^s) \quad (6)$$

So that, the normal unit vector and the *n* and *s* superscripts respectively represent normal and shear components.

The maximum pressure among the particles p_{max}, is determined using Eqs. (7) and (8) considering the contact surface radios of a and normal force of f^n [33]

$$p_{max} = \frac{3f^n}{2\pi a^2} \quad (7)$$

If there is no adherence,

$$f^n = \frac{4E_{eq}}{3R_{eq}} a^3 \quad (8)$$

where E_{eq} and R_{eq} respectively are the equivalent elastic module and the equivalent radios. The total normal displacement is also obtained from Eq. (9)

$$\delta^n = \frac{a^2}{R_{eq}} \quad (9)$$

The following equation (Eq. (10)) is established between the normal force and displacements

$$f^n = -K^n(\delta^n)^{3/2} \quad (10)$$

Also, the normal elastic constant K^n from the equivalent parameters of the two adjacent particles is also in Eq. (11)

$$K^n = \frac{4}{3} E_{eq} \sqrt{R_{eq}} \quad (11)$$

True tangent force δ^s is calculated considering the previous tangent force δ^{s0} and tangential displacement changes $\delta^s - \delta^{s0}$by the tangential stiffness (Eq. (12) and Eq. (13).

$$f^s = f^{s0} + K^s(\delta^s - \delta^{s0}) \quad (12)$$

$$K^s = K^{s0}\left(1 - \frac{\frac{2}{3}K^{s0}\delta^s}{\mu f^n}\right)^{1/2} \quad (13)$$

where μ is the friction coefficient. With the equivalent shear stiffness of E_{eq}, equivalent radius of R_{eq} and the true normal displacement of δ^n we have

$$K^{s0} = 8G_{eq}\sqrt{R_{eq}\delta^n} \quad (14)$$

in another way, since the stress-displacement relation in the true normal force is uniqe, we have

$$K^s = K^{s0}\left(1 - \frac{f^s}{\mu f^n}\right)^{1/3} \quad (15)$$

$$K^s = 8G_{eq}\theta\delta^n \pm \mu(1-\theta)\frac{\Delta f^n}{\Delta \delta^n} \quad (16)$$

where the negative sign is for loading conditions. Whenever $|F^s| \le \mu|F^n|$, the θ parameter will equal 1. The maximum tangential stress limit in fact follows the Coulomb's Friction Law.

$$|F^s| \le \mu|F^n| \quad (17)$$

In the above equations, the equal normal and shear stiffness constants are determined through the Eq. (18) and Eq. (19)

$$\frac{1}{E_{eq}} = \frac{1-\nu_i^2}{E_i} + \frac{1-\nu_j^2}{E_j} \quad (18)$$

$$\frac{1}{G_{eq}} = \frac{2-\upsilon_i}{G_i} + \frac{2-\upsilon_j}{G_j} \quad (19)$$

4. Numerical Analysis

4.1. Modelling Conditions

In this study, Itasca PFC3D version 5 software was used to investigate the strsee-displacement variation of the sand in different particle sizes. This software is a discrete element method code which models the particles and borders based on definition of the balls and the walls. The commnds required for madelling are applicable using the FISH programming language [34]. In modelling, the particles are considered in rigid form but can overlap.

4.2 Input Parameters

In modelling the plate load test on a sandy soil under staged loading, a small scale sample is used to reduce the computational time. Thus, the space size of the model is 100 (length), 100 (width) and 110 (height) mm and the foundation is a square with a side about 8.16 mm (Figure 2) which however, height of the sample will be lower than height of the container after reaching the equilibrium. Number of the balls used in each modelling condition has been determined based on size of the articles and its prosity amount. 27 clamps (mass) has also been used to apply the gravitational load, so that weight of the clams is increased in each stage.

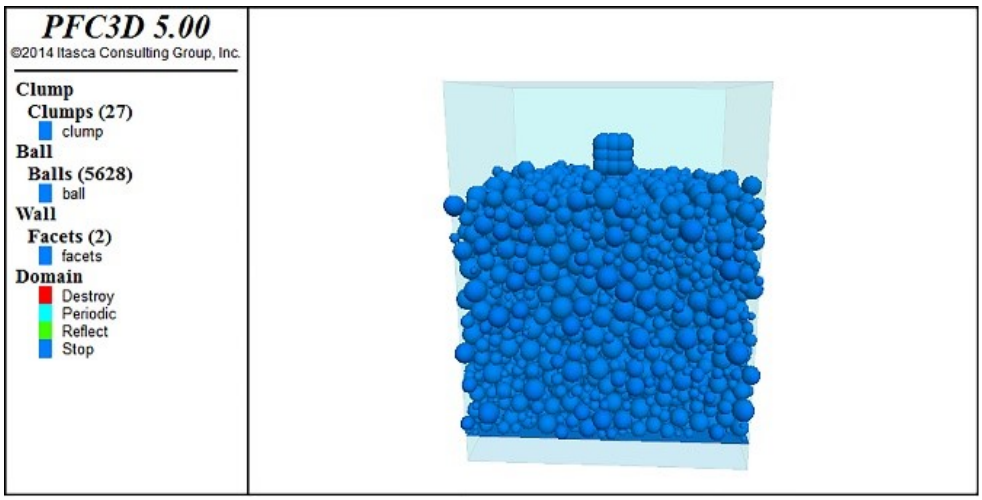

Figure 2. Schematic view of the produced model

The lateral walls are included in form of periodic boundaries and vertical loading is performed after equilibrium of the initial conditions of the sample in stage form. Considering the minimization done, the scale of other parameters and units has been calculated based on the results from Iai et al. [35]. Accordingly, the strain scale factor is determined from the Eq. (20)

$$\mu_\varepsilon = \mu \left(\frac{(V_s)_m}{(V_s)_p}\right)^2 \quad (20)$$

where in, μ is the length scale factor and $(V_s)_m$ and $(V_s)_p$ are shear wave velocity of earth deposits respectively for the model and the actual conditions considered for model testing on loose sand $\mu_\varepsilon = 1$ according to the recommendation of Iai et al. [34]. In this way, μ length scale factor, density μ_ρ and strain μ_ε have been considered to be 1/6, 1 and 1, respectively. By applying these factors, the values used in input parameters are given in form of Table 1. The normal stiffness value, based on the measurement values and the performed calibration has been considered by Ahmadi et al. [35] for Anzali Sand and applied for all samples with similar density indexes in equal form, in order to study the influence of particle size.

Table 1. Input parameters for DEM simulation

Parameter	Value
Assembly of particles	
Diameter	variable
Normal stiffness	5×10^5 N/m
Shear stiffness	5×10^5 N/m
Normal critical damping ratio	0.1
Shear critical damping ratio	0.0
Friction coefficient	5.0
Density	2660 kg/cm^3
Porosity	0.38 to 0.43
Boundary conditions (walls)	
Normal stiffness	10^{10} N/m
Shear stiffness	10^{10} N/m
Friction coefficient	0.5

5. Laboratory Evaluation

5.1. Laboratory Equipments

The device used to perform a static loading test , in order to assess the sand settlement conditions, includes a rigid and cube-shaped box maesuring 60 × 60 cm in the plan and about 60 cm height located on a steel frame. One side of the cubic box is made of a plexiglass plate and in transparent form. A hydroloc loading jack is installed on the device to apply vertical load which includes a vertical displacement gauge (LVDT) to measure the magnitude of the deformation in the sample level. Force exercise planning has been done in a way that the test can be carried out both by stress control and strain control. In these tests, loading was performed in form of strain control. The device includes a digital data logger which can record the load values and deformations. The lower plate for applying uniform stress to the sample is square-shaped, completely rigid with a 10×10 size in the plan. Figure 3 shows a view of the loading box used in this study.

Figure 3. Image of the loading box apparatus

5.2. Characteristics of Soil

This study has used Anzali sand as a criterion of geotechnical parameters in numerical modelling. The major soils forming Anzali are the fine-aggregated and uniform sand. The geotechnical studies carried out in many of these

areas have confirmed this issue to a great depth [36]. The existing sand are generally quiet uniform, fine-aggregated to very fine-aggregated with a densification from loose to medium. This has been confirmed According to the geotechnical studies conducted in many of these areas and to a great depth. It can be said that the typical Anzali sand has a D50 around 0.2 to 0.3 mm and in a bad-aggregated form, it includes a very narrow range of particle size. Also, studies on shear strenght of Anzali sand showed that for a clean sand with solidation stress of 150 kPa, the friction angle corresponding to the steady state resistence is about 30 degrees which is decreased with a 20 percent increase in amount of fine-aggregated material (silt) by about 26 degrees. The soil used is a relatively uniform fine-aggregated sand of Anzali which has typically covered many of the subsurface layers in coastal city of Anzali. Sand aggregation has been shown in Figure 4 and typical specifications of the soil used in the tests are shown in Table 2.

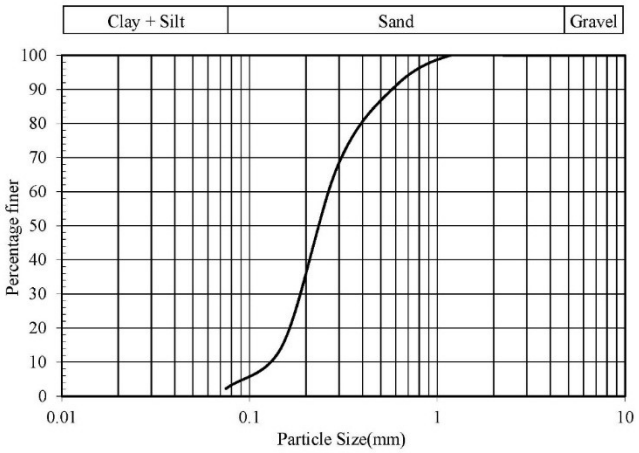

Figure 4. Grain size distribution of Anzali sand

Table 2. Some specifications of Anzali sand

Parameter	Value
Classification (USCS)	SP
Coefficient of uniformity (Cu)	2.28
Coefficient of curvature (Cc)	1.11
Specific gravity (Gs)	2.66
Maximum void ratio (e_{max})	0.83
Minimum void ratio (e_{min})	0.57
Average grain size (D_{50})	0.24mm
Effective grain size (D_{10})	0.12mm

5.3. Comparison of Laboratory Results and Numerical Simulation

In order to verify the accuracy of the results obtained from numarical modeling, the results of loading the laboratory plate performed on Anzali sand was compared to similar conditions simulated by PFC3D. Figure 5 shows the comparison of the results obtained from numerical simulation of Anzali sand under gravity loading by the discrete element method with the results tested on Anzali sand by a physical modeling apparatus. The sand density condition has been applied to the laboratory sample in a loos condition, with a relative density of about 30 percents for the sample and similarly, a porosity around 0.42 is considered in DEM analysis. Comparison of the results shows that the applied method has a good accuracy for predicting stress-displacement behaviour of the sandy soil.

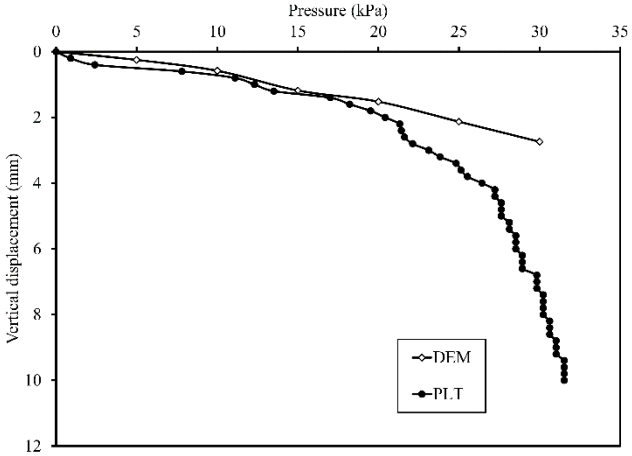

Figure 5. Comparison of laboratory results and numerical simulation on loose sand

6. Analysis of the Results

In order to investigate the effect of size on the modulus of subgrade reaction, the modelling has been done in two aggregation modes and each in two conditions of loos and dense. In the first stage, only the aggregates with the same size were used. Based on the scale used for Anzali sand, in this case, real size of the sand has been considered 0.2, 0.5, 1.0 and 1.5 mm and has been simulated with the same previous scale in PFC3D. In the latter case, the aggregates are considered relatively uniform and for aggregation ranges in sizes of 0.1 to 0.3, 0.3 to 0.50, 0.4 to 0.8 and 0.8 to 1.6 mm. In loose conditions, the samples are made with a porosity of *n=0.38*. Table 3 shows the size characteristics of each sample and also the number of particles obtained in different conditions in the simulation.

The results from modeling the samples have been shown in form of a stress variation diagram based on vertical displacement of the loading plate in Figures 6 and 7 for the samples with completely identical sizes and Figures 8 and 9 for the samples with relatively uniform dimensions. Considering the loading in simulation, DEM has been done in form of stress control (stepwise stress). As expected, the samples with lower hollowwness (*n=0.38*) have had the ability of larger loads and in loos samples with less stresss the sample has become unstable.

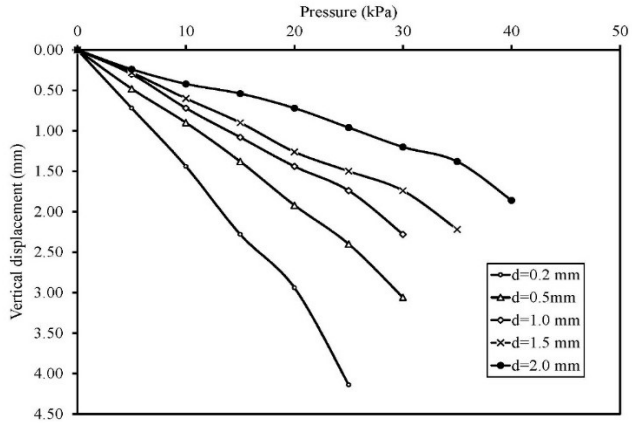

Figure 6. Variations of stress-displacement for completely equal sizes on loose condition from DEM

Table 3. Size characteristics of samples for DEM analysis

Sample No.	Particle size property	Real size (mm)	Particle size in model(mm)	Apparent Density	Number of particles
1	equal size	0.2	0.6	Loose	533986
2	equal size	0.5	1.5	Loose	34175
3	equal size	1	3.0	Loose	4271
4	equal size	1.5	4.5	Loose	1265
5	equal size	0.2	0.6	Dense	561606
6	equal size	0.5	1.5	Dense	35942
7	equal size	1	3.0	Dense	4492
8	equal size	1.5	4.5	Dense	1331
9	relatively uniform	0.1 – 0.3	0.3 – 0.9	Loose	426381
10	relatively uniform	0.3 – 0.5	0.9 – 1.5	Loose	62778
11	relatively uniform	0.4 – 0.8	1.2 – 2.4	Loose	17834
12	relatively uniform	0.8 – 1.6	2.4 – 4.8	Loose	2227
13	relatively uniform	0.1 – 0.3	0.3 – 0.9	Dense	449349
14	relatively uniform	0.3 – 0.5	0.9 – 1.5	Dense	65845
15	relatively uniform	0.4 – 0.8	1.2 – 2.4	Dense	18665
16	relatively uniform	0.8 – 1.6	2.4 – 4.8	Dense	2324

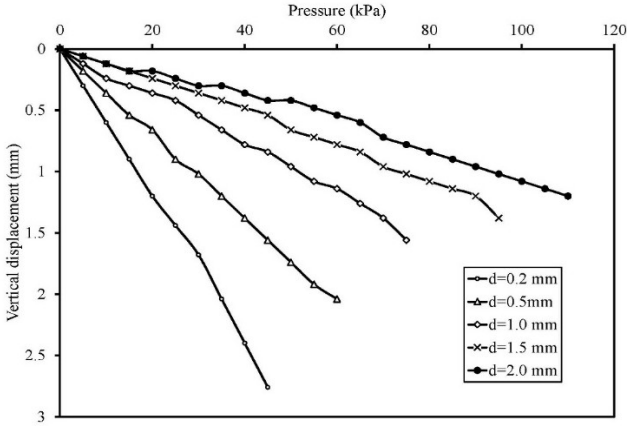

Figure 7. Variations of stress-displacement for completely equal sizes on dense condition from DEM

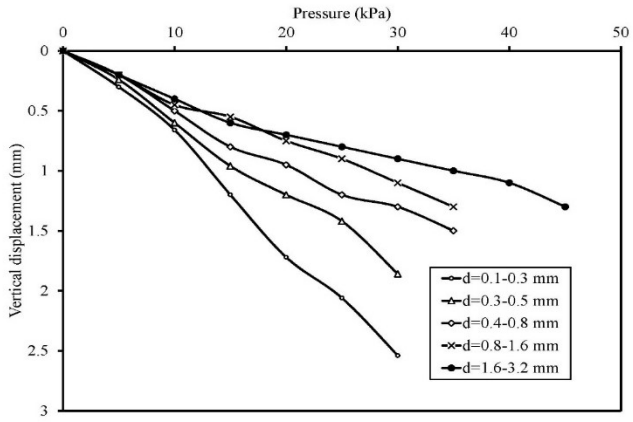

Figure 8. Variations of stress-displacement for relatively uniform sizes on loose condition from DEM

Based on definition of subgrade reaction modulus, gradient of the stress-displacement diagram has been determined, the results of which for different samples are shown in figures 10 and 11, respectively for the samples with quit similar sizes and samples with relatively similar sizes. Based on the obtained results, in samples with quite equal sizes, increase in size of the aggregates from 0.2 mm to 1.5 mm results in a 2.5 fold increase in K_s. In semi-uniform fine-aggregated samples with aggregation interval, by growth in medium size of the particles from 0.2 to 1.2 mm we observe a 5-fold increase in K_s for dense conditions. Also, the results show that although in both cases, increase in size of the aggregates results in increase in amount of subgrade reaction modulus, process of this increase is different in various situations. For the samples with completely equal sizes, a relatively linear relationship can be observed among K_s and the particle diameter (d). Although various fittings have shown that K_s variations with particle diameter (d) for the samples with completely equal sizes in form of a exponential function have higher correlation coefficients but up to a size around 1.5 mm, linear relationship has also a high correlation. However, in relatively uniform fine-aggregated samples with a aggregation interval, the relationship among increase in K_s with average particle diameter (d_m) is not linear and has a roughly logarithmic process. Table 4 shows the fited relationships for different granulation and consendation conditions and also the correlation coefficients for each one. In these relationships, K_s is based on KPa/mm and d and dm are based on mm. Therefore, it is expected that in addition to the fact that size of the particles is a very effective paraemeter in soil stiffness under axial loading, aggregate distribution can also have a decisive role in value of this parameter. Since size of the sand particles in nature is not quite equal and uasually has a granulation interval (although limitted), it is expected that variations of subgrade reaction modulus based on medium particle size have an upward and linear process and especially in the samples with a higher relative density, intensity of these variations will be more in fine-aggregated samples.

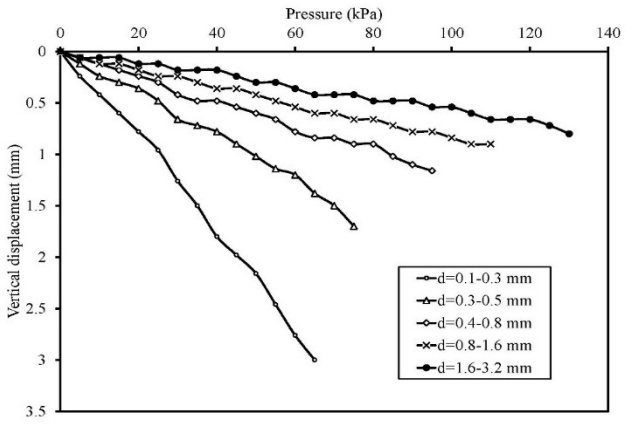

Figure 9. Variations of stress-displacement for relatively uniform sizes on dense condition from DEM

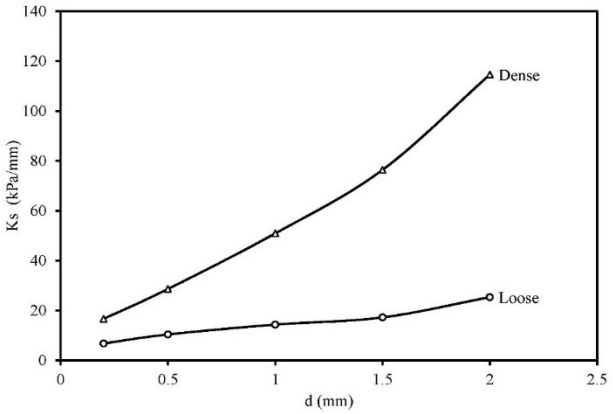

Figure 10. Variations of subgrade reaction modulus with particle size for completely equal sizes on loose and dense condition

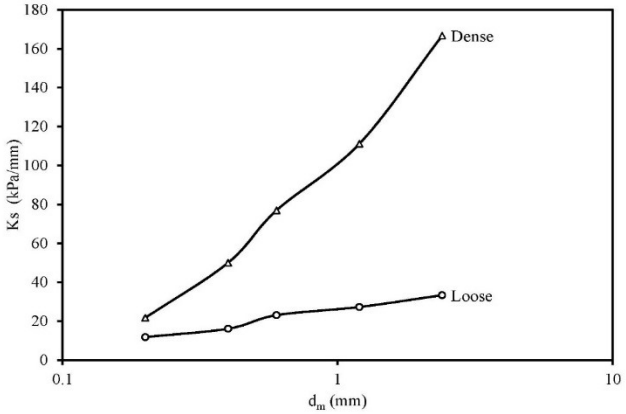

Figure 11. Variations of subgrade reaction modulus with particle size for relatively uniform sizes on loose and dense condition

Table 4. Curve fitting results from DEM for Ks determination

Particle size property	Apparent Density	Curve Fit Equation	R^2
Equal size	Loose	$K_s = 9.55d + 4.90$	0.96
Equal size	Dense	$K_s = 83.23d + 8.36$	0.93
Relatively uniform	Loose	$K_s = 8.83\ln(d_m) + 25.82$	0.90
Relatively uniform	Dense	$K_s = 57.95\ln(d_m) + 108.22$	0.90

7. Conclusion

The present research has investigated the variations of the subgrade reaction modulus in fine-aggregated and relatively fine-aggregated sand with uniform or relatively uniform aggregates through numerical simulation of the plate load test using the discrete element method.

The results show that the size of the particles have a significant effect on amount of the subgrade reaction modulus for similar density conditions. K_s variations based on the particle size in completely equal samples has shown a relatively upward linear process, while by increase in granulation range, these changes will have a non-linear form; especially in high relative density (low porosity) condition, a more severe impact is observed in rate of subgrade reaction modulus.

References

[1] A. Eslami, Foundation engineering design and construction, Building and Housing Research Center, BHRC. No. B-437, Tehran, 2006.

[2] H.G. Poulos, Methods of Analysis of Piled Raft Foundations, a Report Prepared on Behalf of Technical Committee TC18 on Piled Foundations, International Society of Soil Mechanics and Geotechnical Eng., the University of Sydney, Australia, 2001.

[3] M.A Biot, Bending of an Infinite Beam on an Elastic Foundation, Journal of Applied Physics 12 (1937) 155–164.

[4] K. Terzaghi, Evaluation of Coefficient of Subgrade Reaction, Geotechnique 5 (1955) 297–326.

[5] A.P.S. Selvadurai, Elastic Analysis of Soil-Foundation Interaction, Developments in Geotechnical Engineering 17 (1979) 7–9.

[6] S. Vesic, Beam on elastic subgrade and the Winkler hypothesis. Proceedings of the 5th International Conference of Soil Mechanics and Foundation Engineerin, Paris (1961).

[7] H.M. Makhlouf, J.J. Stewart, Factors influencing the modulus of elasticity of dry sand. Proceedings of the 6th International Conference of Soil Mechanics and Foundation Engineering, Toronto, Canada, 1 (1965) 298–302.

[8] B. Okeagu, G. Abdel-Sayed, Coefficients of Soil Reaction for Buried Flexible Conduits, Journal of Geotechnical Engineering 110 (1984) 908–922.

[9] N.F. Ismael, Coefficient of Subgrade Reaction for Footings on Desert Sands, Transportation Research Board Business Office, Washington, USA, Research Record No. 1137 (1987) 82–89.

[10] P.S. Lin, L.W. Yang, H. Juang, Subgrade reaction and load-settlement characteristics of gravelly cobble deposits by plate-load tests, Canadian Geotechnical Journal 35 (1998) 801–810.

[11] A.T. Daloglu, C.V.G. Vallabhan, Values of K for slab on Winkler foundation, Journal of Geotechnical and Geoenvironmental Engineering 126 (2000) 463-71.

[12] R.Z. Moayedi, S.A. Naeini, Evaluation of modulus of subgrade reaction (Ks) in gravely soils based on SPT results, IAEG2006 Paper number 505, The Geological Society of London (2006).

[13] A. Dey, P.K. Basudhar, Flexural Response of Footing on Reinforced Granular Beds of Variable Subgrade Modulus, International Journal of Geotechnical Engineering 2 (2008)199 – 214.

[14] S.Y. Meshkat, Evaluation of size and direction effect on subgrade reaction modulus by Plate Load Test, MSc. thesis, Sharif University of Technology, 2008.

[15] M.M. Ahmadi, Y. Meshkat, An investigation on the dependence of coefficient of subgrade modulus on width of footings and direction of loading for Tehran soil using plate load test. Proceedings of Fourth National Congress on Civil Engineering, University of Tehran (4NCCE), Tehran, Iran (2008).

[16] P. A. Cundall, A computer model for simulating progressive, large-scale movements in blocky rock systems, Proc. Symp. Znt. Sot. Rock Mech., Nancy (1971).

[17] P.A. Cundall, O.D.L. Strack, A discrete numerical model for granular assemblies, Geotechnique 29 (1979) 47–65.

[18] Thornton, L. Zhang, Numerical Simulations of the Direct Shear Test, Chemical Engineering & Technology 26 (2003) 153–156.

[19] J. Wang, M. Gutierrez, Discrete element simulations of direct shear specimen scale effects, Geotechnique 60 (2010) 395–409.

[20] M. Hazeghian, A. Soroush, DEM simulation of reverse faulting through sands with the aid of GPU computing, Computers and Geotechnics 66 (2015) 253–263.

[21] L. Cui, C. O'Sullivan, S. O'Neill, An analysis of the triaxial apparatus using a mixed boundary three-dimensional discrete element model, Geotechnique 57 (2007) 831–844.

[22] J. de Bono, G. McDowell, D. Wanatowski, Discrete element modelling of a flexible membrane for triaxial testing of granular material at high pressures, Géotechnique Letters 2 (2012) 199–203.

[23] S.A.G. Torres, D.M. Pedroso, D. J. Williams, H.B. Mühlhaus, Strength of non-spherical particles with anisotropic geometries under triaxial and shearing loading configurations, Granular Matter 15 (2013) 531–542.

[24] N.S. Nguyen, S. François, G. Degrande, Discrete modeling of strain accumulation in granular soils under low amplitude cyclic loading, Computers and Geotechnics 62 (2014) 232–243.

[25] M. Hu, C. O'Sullivan, R.R. Jardine, M. Jiang, Study on the Deformation of Loose Sand under Cyclic Loading by DEM simulation. GeoShanghai 2010 International Conference, Shanghai, June 3–5 (2010).

[26] N. Ravichandran, B. Machmer, H. Krishnapillai, K. Meguro, Micro-scale modeling of saturated sandy soil behavior subjected to cyclic loading, Soil Dynamics and Earthquake Engineering 30 (2010) 1212–1225.

[27] J. de Bono, G. McDowell, An insight into the yielding and normal compression of sand with irregularly-shaped particles using DEM, Powder Technology 271 (2015) 270–277.

[28] M. Jiang, A. Murakami, Distinct element method analyses of idealized bonded-granulate cut slope, Granular Matter 14 (2012) 393–410.

[29] P.W. Cleary, DEM simulation of industrial particle flows: case studies of dragline excavators, mixing in tumblers and centrifugal mills, Powder Technology 109 (2000) 83–104.

[30] U. El Shamy and N. Zamani, Discrete element method simulations of the seismic response of shallow foundations including soil-foundation-structure interaction, International Journal for Numerical and Analytical Methods in Geomechanics 36 (2011) 1303–1329.

[31] R.M. O'Connor, J.R. Torczynski, D.S. Preece, J.T. Klosek, J.R. Williams, Discrete element modeling of sand production, International Journal of Rock Mechanics and Mining Sciences 34 (1997) 3–4.

[32] G. Lian, C. Thornton and D. Kafui, Trubal: A 3-D computer program for modeling particle assemblies. Aston university, 1994.

[33] K.L. Johnson, Contact Mechanics. Cambridge University Press, 1985.

[34] Itasca Particle Flow Code, PFC3D, ver 5.00, Itasca Consulting Group, Inc (2014).

[35] S. Iai, T. Tobita, T. Nakahara, Generalised scaling relations for dynamic centrifuge tests, Geotechnique 55 (2005) 355–362.

[36] H. Ahmadi, A. Eslami, M. Arabani, Characterization of sedimentary Anzali sand for static and seismic studies purposes, International Journal of Geography and Geology 4 (2015) 155–169.